© 1997 The Chemical Society of Japan

Excitation Energy Dependence of Transient Absorptions of [*N*,*N'*-*o*-Phenylenebis(salicylideneaminato)]cobalt(II) in Dmf Solution

Yukako Ohashi

Department of Chemistry, Faculty of Education, Bunkyo University, Minamiogishima, Koshigaya, Saitama 343

(Received December 26, 1996)

[*N*, *N'*-*o*-Phenylenebis(salicylideneaminato)]cobalt(II), [Co(saloph)], forms two solvated complexes in the dmf solution; that is [Co(saloph)]·dmf at higher temperature and [Co(saloph)]·2dmf at lower temperature. The transient absorptions of the two species were measured in the present work with irradiation of the 532 nm- and 355 nm-light. For [Co(saloph)]·2dmf, the intensity change of the transient absorption induced by the 532 nm-excitation was ca. 5 times larger than that induced by the 355 nm-excitation, although the spectra was the same. By contrast, for the transient absorption of [Co(saloph)]·dmf, no dependence on the excitation wavelength was found with respect to the spectra, the absorption intensity or the decay rates. A quantum calculation of the electronic excited states was carried out by ZINDO model. Taking into consideration the calculated results, the observed differences between the excitation-wavelength dependence of the transient absorptions are discussed.

The Schiff-base complexes of the cobalt(II) ion, CoL, have been known to react reversibly at the metal center with small molecules such as O_2, NO, and CO_2.[1)] Though the first study of the reversible binding between the cobalt(II) ion and the molecular oxygen was reported in the crystalline state,[1a)] most of these reactions have been investigated in solution. In these reactions, it has been supposed that the first step to the oxygenation reactions is an axial coordination of a strong electron donor to the cobalt ion.[1b,2)] Though *N*,*N*-dimethylformamide (dmf) was frequently used as a solvent for these reactions, in several experiments of the dmf solutions of CoL the oxygenation reactions occurred without addition of any other electron donor. In the solutions the dmf–CoL interaction was not found spectroscopically, but the formation of the very weak dmf adduct was assumed in the reaction processes.[2)] The weak solvation to the metal center frequently plays an important role at the initial step and exerts large influence on the chemical reactivity. Therefore, we intended to investigate the effect of weak dmf solvation to CoL from the aspect of the electronic structures using spectroscopic methods.[3,4)]

With respect to such metal complexes of planar π-electron ligands, the electronic structures accept great influence by non-planar deformation of the ligands, which makes it quite difficult to discuss the solvation effect on the electronic states. Though [*N*,*N'*-ethylenebis(salicylideneaminato)]-cobalt(II) ([Co(salen)]) has been extensively investigated in these oxygenation reactions, we adopted [Co(saloph)] (Chart 1) as a material due to the planarity of the adduct structure. The molecular structures of the axial adducts of [Co(salen)], that is [Co(salen)]·X, have been reported to deviate considerably from the plane by forming the adducts.[5)] On the other hand, the imidazole adduct of [Co(saloph)] was reported to maintain the planar structure.[6)] In the previous study of [Co(saloph)] in dmf, we measured the ^{1}H NMR chemical shifts, the UV-vis absorption spectra, the cyclic voltamogram and the preliminary spectra of the laser-induced transient absorption.[4)] From the observed results, the existence of the three solvated species was confirmed in the ground state; the paramagnetic 5-coordinated complex ([Co(saloph)]·dmf), the paramagnetic 6-coordinated complex ([Co(saloph)]·2dmf) and the antiferromagnetic dimer.

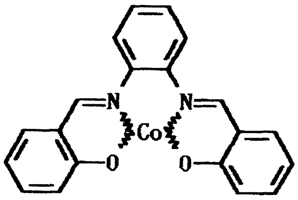

Chart 1. [Co(saloph)].

In the present study, we measured the transient spectra by using the 355 nm- and 532 nm-light of a Nd : YAG laser for [Co(saloph)]·dmf and [Co(saloph)]·2dmf at various temperatures in order to investigate the energy relaxation path. For [Co(saloph)]·2dmf, the intensity of the transient absorption depended on the excitation wavelength, but for [Co(saloph)]·dmf no dependence was observed. In order to relate these differences with the electronic structures, a molecular calculation was carried out by ZINDO model. The solvation effect on the dd transition energies was found to be large for such weak solvation, which was considered as a principal cause for the above difference regarding the transient absorptions

Experimental

Materials. [Co(saloph)][7)] and [Ni(saloph)][8)] were synthesized following the references. Dmf of luminescent grade was used and dried with molecular sieves 4A 1/16. The solution of 5×10^{-4}

mol dm^{-3} were prepared under nitrogen atmosphere by using the solvents purged for 30 min with the nitrogen gas dried through sulfuric acid.

Apparatus. The difference spectra of the transient absorption were measured in a 2 mm quartz cell using an excitation by a Nd : YAG laser (Continuum Surelite II-10, 650 mJ/pulse at 1.06 μm) and monitored from the transverse direction by a pulsed xenon lamp. The detection by a storagescope (Iwatsu TS-8123) and scanning of a monochromator were controlled by a personal-computer program. The saturation of the absorption intensity of the transient absorption was attained at the laser power above 80 mJ/pulse for the 532 nm-light and 30 mJ/pulse for the 355 nm-light. To avoid decomposition of the complexes, the laser power was controlled at the lowest level in the saturation range. The temperature was varied by using a dry ice-acetone bath. The same experiment was carried out for the dmf solution of paramagnetic [Co(saloph)]•dmf, [Co(saloph)]•2dmf, and diamagnetic [Ni(saloph)].

Calculations of Electronic Structures. We calculated the transition energy and the oscillator strength by the use of the Zerner's Intermediate Neglect of Differential Overlap program[9] (ZINDO) of the CAChe WorkSystem. For [Co(saloph)]•dmf and [Co(saloph)]•2dmf, a spin restricted open shell Hartree–Fock calculation was applied. In order to examine the availability of the 3d atomic parameter used in the program, the electronic states of diamagnetic [Ni(saloph)] were also calculated by a closed shell restricted Hartree–Fock type method.

Results

1. Transient Absorptions of [Co(saloph)]•2dmf by 532 nm- and 355 nm-Excitation at −50 °C. In the previous work of [Co(saloph)] in dmf, we measured the temperature dependence of the UV-vis absorption spectra (Fig. 1a) and determined the thermodynamic constants of an equilibrium (1) between [Co(saloph)]•dmf (stable at higher temperature) and [Co(saloph)]•2dmf (stable at lower temperature) in the 5×10^{-4}—10^{-3} mol dm^{-3} dmf solutions.[4]

$$[\mathrm{Co(saloph)}]\cdot\mathrm{dmf}+\mathrm{dmf}\rightleftarrows[\mathrm{Co(saloph)}]\cdot2\mathrm{dmf}. \qquad (1)$$

In the present experiments, all the measurements were carried out in the concentration of 5×10^{-4} mol dm^{-3}. From the analysis of the equilibrium, the predominant species was attributed to [Co(saloph)]•2dmf near −50 °C. Then we measured the difference spectra of the transient absorption at −50 °C by the 532 nm- and 355 nm-excitation (Figs. 1b and 1c). Hereafter, ΔOD denotes the difference of the absorbance following the excitation. In these spectra, ΔOD=0 was found at the wavelength of ca. 400 nm, 450 nm, and 530 nm, where the isosbestic points in the ground-state spectra were found. Therefore the transient absorption was assigned to the dmf-dissociation process from [Co(saloph)]•2dmf to [Co(saloph)]•dmf.

In Fig. 1b of the 532 nm-excitation, the absorption intensity at 0 μs decreased by 0.16—0.20 at 485 nm at the power attaining the absorbance-saturation. From the values of the concentration (5×10^{-4} mol dm^{-3}) and the optical path (2 mm), it resulted in the change of the molecular extinction coefficient of ca. 2×10^3 mol^{-1} dm^3 cm^{-1}. Regarding the ground state, the molecular extinction coefficient decreased by 4×10^3 mol^{-1} dm^3 cm^{-1} at 485 nm from [Co(saloph)]•2dmf to [Co(saloph)]•dmf. Therefore, the preliminary value of the quantum yield of the photoinduced dmf-dissociation was ca. 0.5 for the 532 nm-excitation.

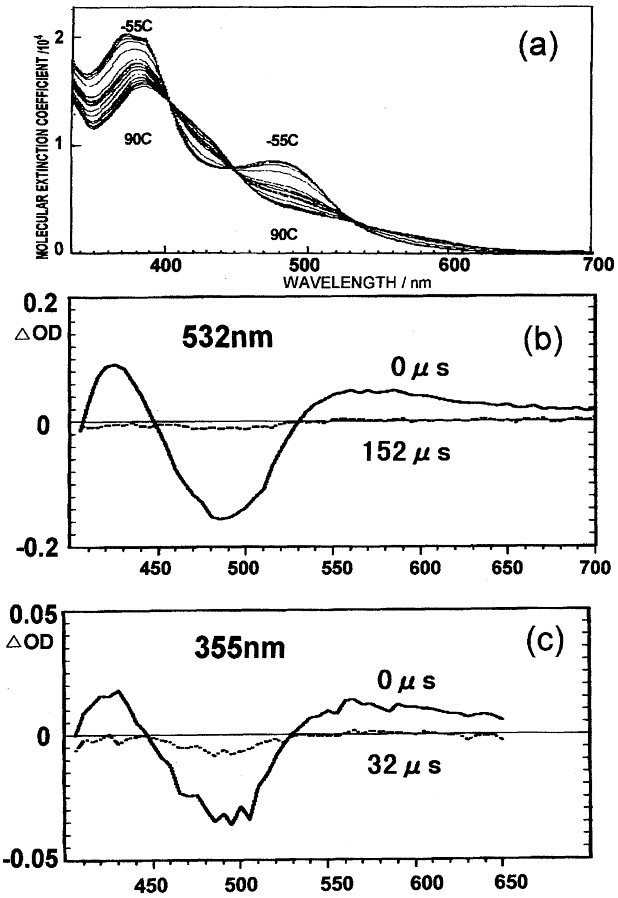

Fig. 1. Ground-state absorption spectra from −55 to 90 °C (a), and time-resolved difference spectra at −50 °C by 532 nm-excitation (b), and by 355 nm-excitation (c) of 5×10^{-4} mol dm^{-3} dmf solution of [Co(saloph)].

Figure 1c shows the transient absorption of [Co(saloph)]•2dmf by the 355 nm-excitation. Comparing it with the absorption for the 532 nm-excitation, the spectrum was the same but the values of ΔOD at 0 μs became smaller by 5.5 times (average for the five experiments). Since all the molecules were excited in the experimental conditions, the quantum yield of dmf-dissociation became less than 0.1 for the 355 nm-excitation. Then it resulted that the transient absorption was attributed to the same dmf-dissociation process but the states absorbing the energy had different electronic character for the 355 nm- and 532 nm-excitation. The decay of the ΔOD values exhibited a single exponential curve and the decay rate was 3×10^4 s^{-1} for both of the excitations. The rise rate of the transient absorption was not observed within the experimental resolution (ca. 10 ns) and the decay rate could be assigned to the process of [Co(saloph)]•dmf+dmf→[Co(saloph)]•2dmf.

2. Transient Absorption of [Co(saloph)]•dmf by 532 nm- and 355 nm-Excitation at 24 °C. On the basis of the reported thermodynamic data,[4] [Co(saloph)] at 24 °C was estimated to exist as 85% of [Co(saloph)]•dmf and 15% of [Co(saloph)]•2dmf. Figure 2 shows the transient absorptions of [Co(saloph)] in dmf at 24 °C excited by the 532 nm- and 355 nm-light. The laser power was controlled to saturate the absorption intensity, so that the observed spectra were considered as the superposed results of ones due to the [Co(saloph)]•dmf and [Co(saloph)]•2dmf in the above ratio.

The decay of ΔOD exhibited a double-exponential curve and the rate constants were determined as 5×10^5 s^{-1} and ca. 10^3 s^{-1} independent of the excitation wavelength. The rise curve was not observed within the experimental resolution. Referring to the decay rate at low temperature (3×10^4 s^{-1}), the fast-decay component was assigned to the absorption originated from [Co(saloph)]•2dmf. Then the slow-decay band was attributed to the transient absorption due to [Co(saloph)]•dmf. By subtracting the contribution of the slow-decay component from the t=0 spectrum, the spectrum of the fast-component at 0 μs was obtained (the broken line in Fig. 2b), which coincided well with the spectrum of [Co(saloph)]•2dmf.

The broad transient absorptions with the decay rate of 2×10^3 s^{-1} has been reported for [Co(saloph)] in CH_2Cl_2 by the 337 nm-excitation and was assigned to another- type of transient solvated complex formed in the excited state.[10] It was reported that [Co(salen)] had another active site for adduct formation besides the metal ion; $CHCl_3$ and C_2H_5OH bonded at the oxygen atom of salen.[11] Moreover, several types of the transient NO adducts were suggested for [Co(salen)] following irradiation.[1e] Therefore, the slow-component observed could be assigned to another type of transient dmf-adduct and the decay rate of ca. 10^3 s^{-1} was considered as the decomposition rate.

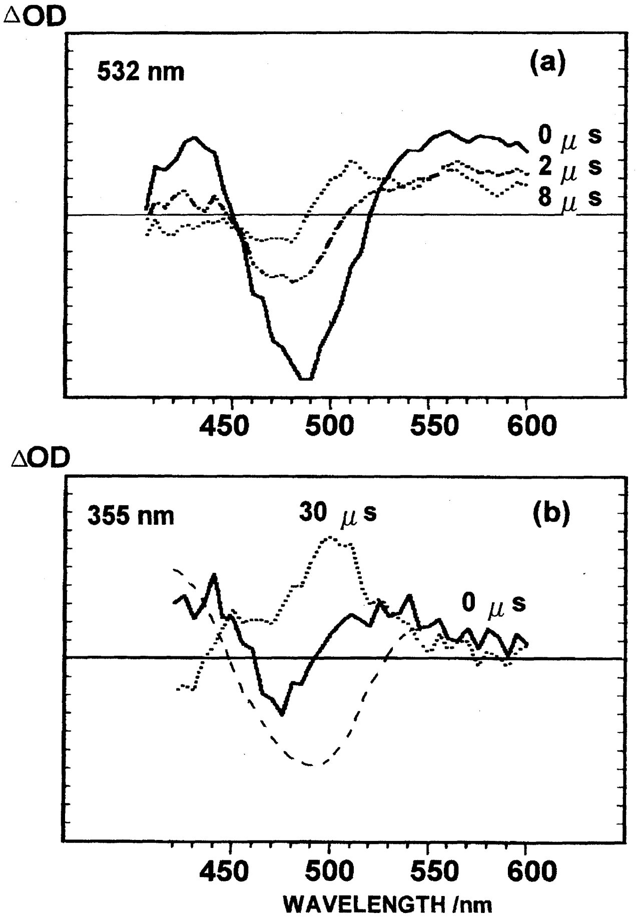

Fig. 2. Time-resolved difference spectra at 24 °C by 532 nm-excitation (a) and by 355 nm-excitation (b) of 5×10^{-4} mol dm^{-3} dmf solution of [Co(saloph)]. A broken line shows the spectrum of the fast-decay component at 0 μs by eliminating the slow-decay contribution.

Generally, the ligand-dissociation was considered to occur in a dd (metal-localized excitation) state. On the other hand, the formation of the above-mentioned adduct at the oxygen atom may be promoted by increase of the electronic density at the oxygen atom in the dπ* or ππ* states. The dd states scarcely interact with the dπ* and ππ* states, so that further discussion of the observed dependence on the excitation wavelength needs the information of the excited electronic structures of the dmf adducts.

Discussion

Availability of ZINDO Model to Saloph Complexes. A semi-empirical ZINDO model (INDO model parametrized for spectroscopy)[7,12] can be applied to the electronic excited states of the metal complexes with unpaired 3d electrons. The restricted Hartree–Fock (RHF) type calculation of ZINDO model was reported to give larger transition energies than the experimental values for the diamagnetic metal complexes.[8,12] Then we first carried out the RHF calculation of the electronic excited states of diamagnetic [Ni(saloph)] in order to examine the availability of the atomic parameters to the saloph complex. Since the UV-vis spectrum of [Ni(saloph)] was similar to that of [Co(saloph)], the calculation of $saloph^{2-}$ and [Ni(saloph)] was carried out by using the reported molecular structure of [Co(saloph)].[13] As is seen in Table 1, the agreement between the calculated and observed results ([Na_2(saloph)] in dmf) was very good for $saloph^{2-}$. The calculated transition energies and oscillator strengths of

Table 1. Calculated Transition Energies (in 1000 cm^{-1}) and Oscillator Strengths (in Parenthesis) of Excited States for $saloph^{2-}$ and [Ni(saloph)], Together with Experimental Data in Dmf Solutions

[Ni(saloph)]		$saloph^{2-}$	
Observed	Calculated	Observed	Calculated
	24.0 (0.01) dd		
	26.5 (0.06) dd		
20.8 (0.15)	27.0 (0.16)	23.0 (0.2)	21.7 (0.27)
	28.0 (0.55)	25.5 (0.5)	24.6 (0.99)
26.7 (0.4)	32.6 (0.36)		
	33.3 (0.37)		
	35.0 (0.35)		
32.3 (0.3)	38.6 (0.17)		
37.1 (0.6)	43.1 (0.31)		
	44.0 (0.25)		
	44.2 (0.25)		

[Ni(saloph)] agreed with the observed spectrum in dmf as a whole, though the energies were higher by 6000—7000 cm^{-1} and the intensities were stronger than the observed values. The dπ^* and $\pi\pi^*$ excited states (denoted hereafter as the π-excited states) interacted easily with each other, so that Table 1 shows only the contribution of the dd transitions to the excited states.

In order to collect more information on the excited states, the transient absorption of [(Ni(saloph)] was measured by the 355 nm- and 532 nm-excitation in the temperature range -50—-5 °C. Independently of excitation-wavelength the broad transient spectrum was observed with the intensity maximum at 430 nm and the molecular extinction coefficient of ca. 25000 $\text{mol}^{-1}\,\text{dm}^3\,\text{cm}^{-1}$ by assuming the complete energy relaxation to the lowest state. The decay rate exhibited a rapid temperature dependence and was formulated as $k/\text{s}^{-1}=6\times10^{14}\exp(-2800/\text{cm}^{-1}/RT)$. From the decay rate, the transient absorption was assigned to a singlet–singlet absorption. Taking account of ca. 7000 cm^{-1} higher shift of the calculated energies, the calculation indicated that the 355 nm ($28.2\times10^3\ \text{cm}^{-1}$)-light excited the π-excited states, and the 532 nm ($18.8\times10^3\ \text{cm}^{-1}$)-light was absorbed in the lower-energy tail of the lowest π-excited state. The rate and intensity of the transient absorption did not depend on the excitation-wavelength, so that the energy relaxation was rapid between the higher and the lowest π-excited states. The observed rapid increase of decay rate with temperature could be interpreted in terms of the energy relaxation to the nearlying dd state.

Analysis of Electronic Excited States of [Co(saloph)]. In the above discussion, ZINDO calculation was shown to be valid for the singlet excited states of the saloph complex. Then we carried out the doublet-state calculation of [Co(saloph)] and the dmf adducts. The first calculation was carried out by using the reported structure of [Co(saloph)]. The calculated and observed results are shown in the first column of Table 2. Taking into consideration of ca. 7000 cm^{-1} deviation of the transition energies for the calculation of [Ni(saloph)], the agreement between the observed peaks (in CH_2Cl_2) and the calculated transition energies was good. The weak transitions at 19.2—$25.6\times10^3\ \text{cm}^{-1}$ corresponded to the π-excited states of triplet-origin, which were intensified through the spin-orbit interaction due to the cobalt(II) ion.

Regarding the calculation for the dmf adducts, the molecular structure must be assumed. The bond length between the cobalt(II) ion and the oxygen atom of dmf was reported as 215 pm for the dmf adducts of [Co(salen)], (dmf)[Co(salen)]O_2 [Co(salen)](dmf).[14)] The other reported value of the Co–O(dmf) distance was 213 pm in the dmf solution of $[\text{Co(dmf)}_6]^{2+}$.[15)] The present dmf adducts of [Co(saloph)] were not isolated as a solid and the spectral change induced by dmf solvation was small, so that we made the calculation by varying the Co–O(dmf) distance from 220 to 300 pm. In the molecular structure of [Co(saloph)] (2-methylimidazole),[6)] the planar ring of imidazole was projected on the linear O–Co–N line of [Co(saloph)] by viewing perpendicular to the [Co(saloph)] plane. The similar steric relation was reported for the O=C–N plane of dmf in the dmf adduct

Table 2. Calculated Transition Energies (in 1000 cm^{-1}) and Observed Data of [Co(saloph)] in CH_2Cl_2, [Co(saloph)]·dmf, and [Co(saloph)]·2dmf in Dmf Oscillator strength less than 10^{-2} was not shown.

[Co(saloph)]		[CoL°]·dmf	[CoL$^{\text{Imd}}$]·dmf	[CoL$^{\text{Imd}}$]· 2dmf	[CoL]·dmf	[CoL]·2dmf
Observed	Calculated	Calculated	Calculated	Calculated	Observed	Observed
8.1 (1×10^{-5})	6.65 dd	8.08, 10.3 dd	8.94, 13.6, 14.8 dd	10.9, 11.2, 13.4 dd		
	7.81 dd	17.4 dd	16.1, 19.5, 19.8 dd	16.1, 17.9, 19.5 dd		
	19.2, 19.6,	18.8, 19.3, 24.0	20.6, 22.3	20.8		
	22.9, 25.6	25.2 (0.01)	23.2 dd	21.6 dd		
	25.8 (0.02) dd		24.8, 26.1, 27.6	20.8, 22.2, 26.4		
17—20 (0.08)	26.2 (0.17)	25.5 (0.16)	27.6 (0.13)	27.3 (0.10)	17—20.4 (0.1)	20.8 (0.2)
	27.2 (0.45)	25.8 (0.32)	30.0 (0.65)	29.3 (0.17) (dd)		
			30.7 (0.17) (dd)	29.7 (0.61)		
23.2 (0.06)	31.3 (0.16)	29.7 (0.13)	34.2 (0.13)	32.6 (0.10)	23.3 (0.12)	26.0
25.6 (0.4)	31.8 (0.26)	29.9 (0.30)	34.5 (0.18)	33.8 (0.08) (dd)	26.3 (0.3)	27.0 (0.4)
	32.5 (0.32)	32.1 (0.32)	35.6 (0.26) (dd)	34.3 (0.25)		
30.0 (0.05)	35.6 (0.10)	35.3 (0.11)	36.5 (0.16)	36.3 (0.10)	30 sh	
33.3 (0.6)	37.9 (0.12)		38.4 (0.11)	36.9 (0.10)	33 (0.24)	
	37.9 (0.12)		40.4 (0.16)	40.0 (0.16)		
	38.3 (0.11)		41.7 (0.13)	40.3 (0.16)		
				40.6 (0.11)		
40.8 (1.1)	42.9 (0.20)	38.0 (0.09)	45.3 (0.22)			
	44.3 (0.45)	41.9 (0.24)	46.9 (0.19)	44.1 (0.23) (dd)	37.7 (1.0)	
	45.1 (0.12)	42.2 (0.36)	48.6 (0.11)	44.2 (0.15)		
	46.0 (0.11)	43.4 (0.15)	49.0 (0.22)	44.7 (0.21) (dd)		
		45.2 (0.13)		49.7 (0.09)		

of [Co(salen)],[14] so this conformation was adopted for the calculation. In fact, the rotation of the dmf molecule around the Co–O axis was confirmed to give little effect on the calculated results. When [Co(saloph)] formed the 2-methylimidazole adduct with the Co–N(Imd) bond of 207 pm, the bond lengths of Co–O (184 pm) and Co–N (187 pm) between the cobalt ion and the saloph ligand increased to 197 pm and 208 pm, but the other bond lengths and the saloph planarity did not change. Similar bond weakening was reported for [Co(salen)]·X with the Co–X bonds of 209—214 pm; the distances of Co–O and Co–N increased from 185 and 185 pm to 190—192 pm and 187—190 pm by adduct formation.[14]

On the basis of these structural data, the calculation of [Co(saloph)]·dmf was carried out by using the reported structures of [Co(saloph)] and [Co(saloph)]·(2-methylimidazole). Hereafter, the corresponding two structures were denoted as [Co(saloph)°] and [Co(saloph)$^{\mathrm{Imd}}$]. We aimed to explain the energy-relaxation path following the 355 nm-excitation, so that we focused the discussion on the energy region lower than 28.2×10^3 cm^{-1}. The calculated results for 220 pm are shown in Table 2; (dd) denotes small dd contribution to the excited state. The transition energies for [Co(saloph)$^{\mathrm{Imd}}$]·dmf were larger by 1400—3000 cm^{-1} than those calculated for [Co(saloph)°]. On the other hand, the calculated energies for [Co(saloph)°]·dmf decreased by 1000—3000 cm^{-1} compared with those of [Co(saloph)°] regarding the π-excited transitions. The lower shift by dmf addition was reasonably accepted, because dmf neutralized the positive charge of the cobalt ion by donating the lone-pair electrons and it resulted in the decrease of the dπ* transition energies. The similar decrease of the calculated transition energies was found for formation of 2dmf-adduct from dmf-adduct. The case of [Co(saloph)$^{\mathrm{Imd}}$] is shown in Table 2. The calculation for the 2dmf-adduct was carried out by locating two dmf molecules at the same distance, because the molecular structure of CoL·2X was not reported.

With respect to [Co(saloph)] and [Co(saloph)]·dmf, the observed ground-state spectra (Table 2) and the laser-induced transient spectra resembled each other. On the other hand, [Co(saloph)]·2dmf had the observed ground-state absorptions shifted to higher-energy side by the second dmf-addition. Therefore, we concluded that [Co(saloph)] and [Co(saloph)]·dmf had similar molecular structure but that the Co–O and Co–N bonds in [Co(saloph)]·2dmf became weaker than the former two species.

Energy-Relaxation Path. Figure 3 shows the calculated transition energies of [Co(saloph)°], [Co(saloph)°]·dmf, [Co(saloph)$^{\mathrm{Imd}}$]·2dmf and [Ni(saloph)]. From the efficiency of the energy relaxation, the π-excited states (the left) and the dd states (the right) are classified into two groups in the figure. The dotted levels are those with the oscillator strengths of less than 0.01. Taking account of ca. 7000 cm^{-1} higher shift of the calculated energies, the 355 nm- and 532 nm-lights corresponded to the energy of ca. 35 and ca. 26×10^3 cm^{-1}.

Concerning [Co(saloph)] and [Co(saloph)]·dmf, the observed transient species were independent of the excitation-wavelength. In the calculated excited states of [Co(saloph)°] and [Co(saloph)°]·dmf, the lowest π-excited state of singlet-origin (straight line) and of triplet-origin (dotted line) showed the largest change of the electron density at the O and N atoms of saloph. The change can promote the formation of such adducts as [Co(salen)]·$CHCl_3$ at the O atom of saloph. At present no direct evidence was obtained about whether the reactive state was of singlet-origin or of triplet-origin. Regarding [Co(saloph)]·2dmf, the observed quantum yield of photoinduced dmf-dissociation was five times larger by the 532 nm-excitation than that by the 355 nm-excitation. As is seen from the calculated results of [Co(saloph)$^{\mathrm{Imd}}$]·2dmf, the dd states interacted with the π-excited states. The 532

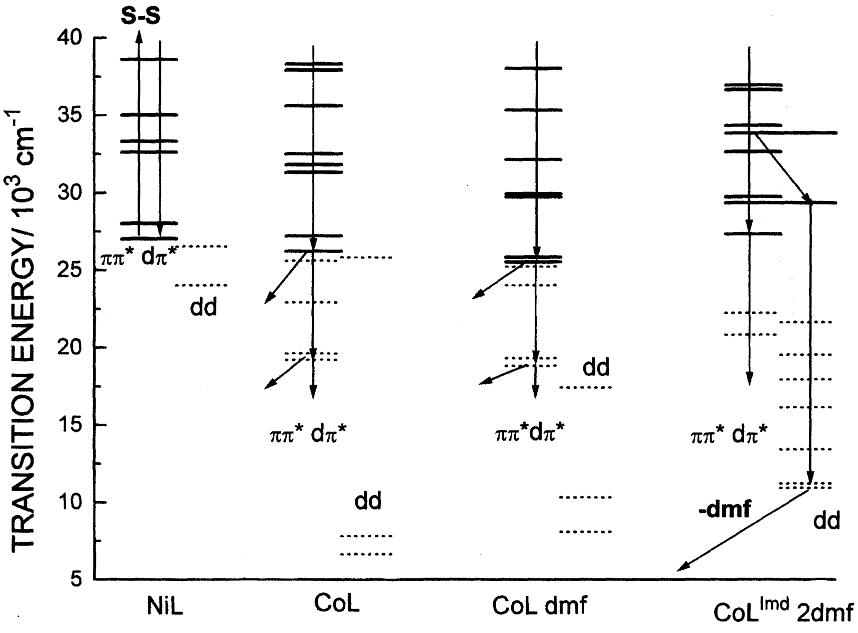

Fig. 3. Calculated Energy Diagram of [Co(saloph)], [Co(saloph)]·dmf, [Co(saloph)Imd]·2dmf, and [Ni(saloph)].

nm-light could excite the low-energy tail of such dd-mixed states (29.3×10^3 cm^{-1}) and then the absorbed energy effectively relaxed to the lowest dd state. On the other hand, the 355 nm-light excited the higher π-excited states. The absorbed energy relaxed predominantly to the lowest π-excited state and partially to the lowest dd state through the higher dd-mixed state. Thus the observed dependence on the excitation-wavelength could be interpreted in terms of the incomplete energy relaxation between the higher π-excited state and the dd state.

Concluding Remarks. It was reported that weak solvation to [Co(saloph)] played a role in the energy relaxation process and that a semiempirical calculation of ZINDO model gave information to explain these results. Though the agreement between the calculated and the observed results was qualitative, the calculation suggested that the Co–O(saloph) and Co–N(saloph) bond became weak following dmf-addition and that such steric deformation changed the interaction between the dd transition and the transitions of π character. This work showed the possibility for a solvent to cause a steric deformation around the metal ion of the metal complexes.

References

1) a) T. Tsumaki, *Bull. Chem. Soc. Jpn*, **13**, 252 (1938); b) N. Bresciani, M. Calligaris, G. Nardin, and L. Randaccio, *J. Chem. Soc., Dalton Trans.*, **1974**, 1606; c) C. Floriani and G. Fachinetti, *J. Chem. Soc., Chem. Commun.*, **1974**, 615; d) R. D. Jones, D. A. Summerville, and F. Basolo, *Chem. Rev.*, **79**, 139 (1979); e) M. Hoshino, R. Konishi, N. Tezuka, I. Ueno, and H. Seki, *J. Phys. Chem.*, **100**, 13569 (1996).

2) E. Cesaroti, M. Gullotti, A. Pasini, and R. Ugo, *J. Chem. Soc., Dalton Trans.*, **1977**, 757.

3) Y. Ohashi and M. Nakamura, *Chem. Lett.*, **1993**, 1389.

4) Y. Ohashi and M. Nakamura, *Bull. Chem. Soc. Jpn.*, **67**, 2921 (1994).

5) N. Bresciani, M. Caligaris, G. Nardin, and L. Randaccio, *J. Chem. Soc., Dalton Trans.*, **1974**, 498.

6) B. J. Kenedy, G. D. Falon, B. M. K. C. Gatehouse, and K. S. Murray, *Inorg. Chem.*, **23**, 580 (1984).

7) D. Chen and A. E. Martell, *Inorg. Chem.*, **26**, 1026 (1987).

8) S. D. Bella, I. Fragala, I. Ledoux, M. A. Diaz-Garcia, P. G. Lacroix, and T. J. Marks, *Chem. Mater.*, **6**, 881 (1994).

9) M. Kotzia, N. Rosch, H. Schroder, and M. C. Zerner, *J. Am. Chem. Soc.*, **111**, 7687 (1989).

10) Y. Ohashi, *Chem. Lett.*, **1990**, 1083.

11) W. P. Schaffer and R. E. March, *Acta Crystallogr., Sect. B*, **B25**, 1675 (1969); G. B. Jameson, F. C. March, W. T. Robinson, and S. S. Koon, *J. Chem. Soc., Dalton Trans.*, **1978**, 185.

12) K. K. Stavrev, M. C. Zener, and T. J. Meyer, *J. Am. Chem. Soc.*, **117**, 8684 (1995); S. D. Bella, I. Fragala, I. Ledoux, and T. J. Marks, *J. Am. Chem. Soc.*, **117**, 9481 (1995).

13) N. B. Pahor, M. Calligaris, P. Delise, G. Dodic, G. Nardin, and L. Randaccio, *J. Chem. Soc., Dalton Trans.*, **1976**, 2478.

14) M. Calligaris, G. Nardin, and L. Ripamonti, *J. Chem. Soc. A*, **1970**, 1069.

15) H. Yokoyama, S. Suzuki, M. Goto, K. Shinozaki, Y. Abe, and S. Ishiguro, *Z. Naturforsch., A*, **50A**, 301 (1995).